
Complexity for deep neural networks and other characteristics of deep feature representations

Romuald A. Janik
Institute of Theoretical Physics
Jagiellonian University
Kraków, Poland
romuald.janik@gmail.com

Przemek Witaszczyk
Institute of Theoretical Physics
Jagiellonian University
Kraków, Poland
przemek.witaszczyk@cern.ch

Abstract

We define a notion of complexity, motivated by considerations of circuit complexity, which quantifies the nonlinearity of the computation of a neural network, as well as a complementary measure of the effective dimension of feature representations. We investigate these observables both for trained networks for various datasets as well as explore their dynamics during training. These observables can be understood in a dual way as uncovering hidden internal structure of the datasets themselves as a function of scale or depth. The entropic character of the proposed notion of complexity should allow to transfer modes of analysis from neuroscience and statistical physics to the domain of artificial neural networks.

1 Introduction

The goal of the present paper is to introduce characterizations of complexity tailored to Deep Neural Networks. In Machine Learning, typically model complexity is associated with the number of model parameters and thus with its potential expressivity. In this work we would like to focus, in contrast, on a notion which captures the complexity of the specific computational task, so that the same neural network architecture with the same total number of parameters could yield differing complexity depending on the dataset on which it was trained.

The motivation for our specific version of complexity comes from the notion of *circuit complexity* in Quantum Information and Physics, although our definition is not a direct translation of that concept to neural networks. Another aspect that we would like to emphasize is that the entropic character of our definition lends itself on the one hand to considerations of efficiency or effectiveness and on the other hand is a direct counterpart of a method of analysis of ensembles spiking neurons in neuroscience [1].

Another goal for the considerations of the present paper is that the proposed definitions could be used to study information processing and feature representations in a deep neural network in a *layer-wise* manner. Intuitively, a (convolutional) deep neural network builds up first local representations (edges/textures) then going further in depth, the features become more nonlocal and more higher-level culminating in the final classification score. The deep convolutional neural network can thus be understood as a highly nontrivial nonlinear *goal directed* analog of a Fourier/wavelet transform of the original image. Similar flavour of analysis is ubiquitous in Physics, where one looks at a system at a progression of scales. This occurs e.g. in the context of (Wilsonian) Renormalization Group, tensor networks or holography (see more in section 2). Thus it is very interesting to introduce *quantitative* characteristics of feature representations at a given scale/layer depth and study their variation as a function of depth.

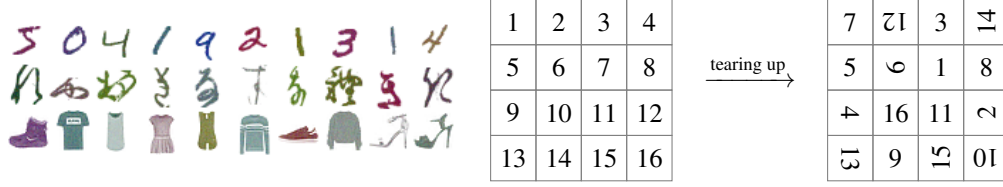


Figure 1: CMNIST, CKMNIST and CFashionMNIST datasets (left). Teared up version (right). See *Supplementary information* for details.

Let us note that this opens up also a quite different theoretical perspective of characterizing, in a nontrivial way, the internal structure at a given scale of a specific dataset or learning task using the trained deep neural network as a *tool* instead of a classifier.

In this respect, as our notion of complexity captures only the nonlinear character of information processing of a given layer, we also introduce a complementary measure – *the effective dimension*, which is sensitive to the details of neurons working in the linear regime.

Naturally, once such notions are introduced, it is interesting to study how these characteristics evolve during training, which may provide both qualitative insight as well as quantitative data for the understanding of the dynamics of deep neural network training.

In order to investigate how the introduced observables differ once one changes the difficulty and type of learning task while keeping the underlying neural network unchanged, we utilize a range of datasets. Since our base network is geared for CIFAR-10, we introduce as drop-in replacements coloured variants of the classical MNIST, KMNIST and FashionMNIST datasets as examples of easier tasks, as well as novel teared-up versions of all these datasets which serve to increase the difficulty of the classification tasks (see Fig. 1 and *Supplementary information*). We also investigate a memorization task, namely CIFAR-10 with random labels [2].

2 Related work and further motivations

The notion of complexity is widespread in both natural and computer science. In the machine learning context there are fundamental ideas on the model and dataset complexities, most prominently the VC dimension and Rademacher complexity. These measure the richness of the class of functions that can be learned by the given algorithm, and in practice play more formal than applied role when dealing with real world problems [3], [4].

More model structure oriented notions are based on circuit complexity [5], [6], where the neural network is treated as a weighted majority, logical or threshold circuit and its expressive power is analysed by e.g. relating network depth to the number of Boolean functions realisable by the network, or its resource usage scaling with input size. This is quite different from what we do, as we aim to quantify the complexity of a *particular* realization of a trained neural network.

In recent years an entirely different perspective emerged with the advent of tensor networks application to machine learning [7], [8]. Tensor networks are a way of representing large matrix multiplication structures of neural networks and play crucial role in quantum physics. They seem to be a bridge connecting starkly different areas of AI, quantum mechanics and much more [9]. In their realm one considers arithmetic complexity [10] of tensor networks, their expressive power [11], [12], and incorporates fundamental concepts of quantum physics, like entanglement, representing correlations at different scales [13], [14], [15], to infer better neural networks design. Even more, one can train models defined directly in tensor network form [16] with accuracy comparable to standard deep neural network structure. Physics based notions of complexity were developed primarily in the continuous setting (see e.g. [17]) but with variants of circuit complexity resurfacing [18]. These developments were fuelled by another view on complexity which emerged from a different direction.

A particularly fascinating thread in theoretical physics is the principle of holography [19], where physical systems are described using an emergent dimension, in which physical features are encoded in a non-local way starting from short-distance to large distance ones (for an analogy with neural networks see [20]). Some of the tensor network constructions mentioned earlier, like MERA, realize

something analogous [21], [22]. In the holographic context, complexity is realized e.g. as spatial volume of the emergent space [23] and thus something additive over holographic scales, which would suggest a corresponding quantity additive over layers in the neural network context.

Both of the above themes motivate us also to investigate *depth-wise* profiles of observables which probe the neural network at various scales and, moreover, to look at the results not only in terms of properties of the given neural network, but also as nontrivial signatures of the structure of the particular dataset/classification task (analogous to a physical system) as a function of scale.

The notion of complexity for neural networks that we propose in the current paper is not a translation of the above concepts but it draws on these intuitions like considerations on gate/operation cost and an additive layer-wise structure.

Finally, let us mention a quite different line of motivation. The entropic character of our definition is grounded in physical considerations, especially in entropic properties of any computational process, and originally inspired by the Landauer principle [24]. In addition, the effective binary variables open up the possibility to use the methods of analysis of ensembles of spiking biological neurons [1], modelled e.g. using a mapping to generalized Ising models [25], where the binary variables play the role of spins. Along these lines, one could use similar methods of analysis based on statistical physics also to the case of deep neural networks. We leave this for future investigation.

3 Comments on convolutional neural networks

Before we describe the proposed observables, we should emphasize the way in which we will treat convolutional layers of a neural network. The individual computational unit of a convolutional layer is a set of C neurons/filters (say of size 3×3). The output of a layer for a batch of N images has dimension $N \times C \times H \times W$. This output arises by passing through the convolutional filters a large number of small 3×3 patches of the output of the previous layer. Thus the neurons in a convolutional layer effectively see a batch of separate $N \cdot H \cdot W$ patches. Since we want to concentrate on analyzing the elementary independent computational units of the convolutional layer, we will always treat the output of the convolutional filters as a huge effective batch of dimension

$$(N \cdot H \cdot W) \times C \quad (1)$$

4 Complexity – entropy of nonlinearity and related notions

The general idea of circuit complexity is to decompose a computation in terms of certain elementary operations (*gates*) and count the minimal number of gates (possibly with an appropriate cost associated to a given gate) necessary to achieve that particular computation up to a given accuracy threshold. We will not implement this prescription for neural networks but rather it will serve us as a heuristic motivation.

One clear point from that definition is that it would not make too much sense to use a gate which, when composed multiple times could be recast just as a single application of such a gate i.e.

$$A_1 \circ A_2 \circ \dots \circ A_n = A \quad (2)$$

An example of such an operation would be a linear map. Hence from *this point of view* it is natural to assume that a linear mapping is trivial and should not contribute to the estimation of complexity.

The most commonly used neuron in current artificial neural networks has a ReLU activation $y = \text{ReLU}(W_i x_i + b)$. Depending on the weights and the inputs, the neuron acts either as a linear function $W_i x_i + b$ when $W_i x_i + b > 0$ or as a zero. In fact both options are trivial under composition. Hence, the complexity of the neuron should be associated with its decision function i.e. it acting sometimes in the linear regime and sometimes clamping the output to zero. To this end, let us introduce

$$z = \theta(W_i x_i + b) \quad (3)$$

where θ is the Heaviside function, so $z = +1$ if the neuron operates in the linear regime and $z = 0$ if the output is set to zero. We will call this binary variable a *nonlinearity variable*. Given the above intuitions, a very natural proposal for the complexity of a single neuron would be the Shannon entropy (measured in bits) of the nonlinearity variable z computed on the dataset

$$H(z) = - \sum_z p(z) \log_2 p(z) \quad (4)$$

which vanishes both for the purely linear and purely turned off regimes. In order to define complexity for a set of neurons (e.g. a layer), we again define a set of binary variables $z_k = \theta(W_{ki}x_i + b_k)$ and define the complexity of the layer as the entropy of the *multidimensional* binary nonlinearity variable

$$complexity = H(Z) = - \sum_{\{z_k\}} p(z_1, \dots, z_C) \log p(z_1, \dots, z_C) \quad (5)$$

This definition captures also the information whether the individual neurons switch their mode of operation independently or not. Let us also note that such a measure is used as an indicator of the information content of ensembles of spiking neurons (which by themselves are naturally binary) in neuroscience (see section 2). A related analogy of the binary variables is with Ising spin variables. This leads to possible neuroscience/physics inspired modes of analysis of artificial neural networks.

Let us note that even for a single layer, the evaluation of (5) is not trivial. In practice, we cannot use entropy estimation based on occurrence counts due to the huge dimensionality 2^C of the space of configurations. In this paper we use, therefore, the method of estimation of entropy from [26] using the xgboost classifier [27] (see *Supplementary information* for more details). Moreover, one should take care with properly interpreting formula (5) in the case of convolutional neural networks. As described in section 3, C is then just the number of channels and *not* the total number of outputs $C \times H \times W$. This makes it feasible to evaluate the entropy for all layers of a resnet-56 network.

For the whole network, one could in principle use exactly the same definition, but that would be impossible to reliably evaluate due to the dimensionality of the configuration space¹. Hence we *define* the complexity of a network by adding up the complexities/entropies of individual layers (see section 2 for further motivation).

$$complexity(network) = \sum_{L \in Layers} H(Z_L) \quad (6)$$

In the present paper, however, we will mostly concentrate on the individual layer complexities $H(Z_L)$ (or their sums over blocks of layers) as a function of depth, training epoch and dataset.

Our definition of complexity is thus essentially the entropy of nonlinearity of the neural network or layer. For other activation functions e.g. for a *sigmoid*, a natural extension would be to define an auxiliary *ternary* variable, corresponding to the three distinct regimes of operation: saturation at 0, approximately linear and saturation at 1, and use again the definition in terms of Shannon entropy.

Derived quantities. It is useful to consider also some other quantities derived from the same data. One natural candidate is the *total correlation* (or multiinformation) between the neurons in a given layer which captures the extent in which the individual neurons switch independently from each other. We will use it in the normalized variant

$$normalized\ total\ correlation = \frac{H(Z_1) + \dots + H(Z_C) - H(Z_1, \dots, Z_C)}{H(Z_1) + \dots + H(Z_C)} \quad (7)$$

Another interesting variable is the average *linearity* of a layer defined by

$$linearity = \frac{1}{C} \sum_{i=1}^C E(Z_i) \quad (8)$$

where $E(Z_i)$ is the expectation value of the nonlinearity variable. The advantage of this quantity is that it is very efficient to compute (at the cost of ignoring correlations) and it distinguishes predominantly linear operation of a neuron from predominantly being turned off, two conditions which are on the same footing and thus indistinguishable from the point of view of entropy. The above suggests, that one should also quantify the properties of the *linear* operation of a neural network layer. In the following section, we will introduce an observable complementary to complexity which aims to do just that.

¹For convolutional networks there would be a further complication due to the different resolutions in various parts of the network and hence different numbers of patches for different groups of layers.

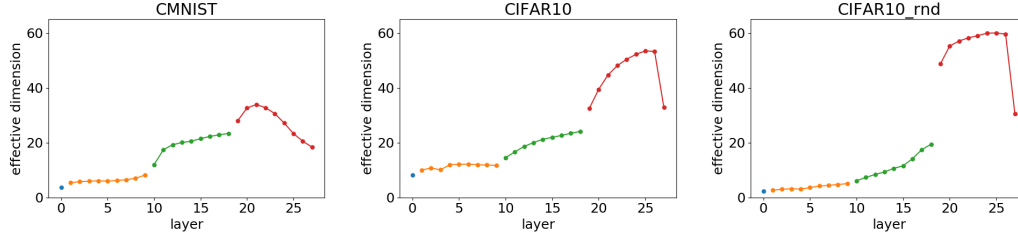


Figure 2: “Holographic” plot of the *effective dimension* as a function of layer depth (topmost ReLUs in residual cells) numbered from the input.

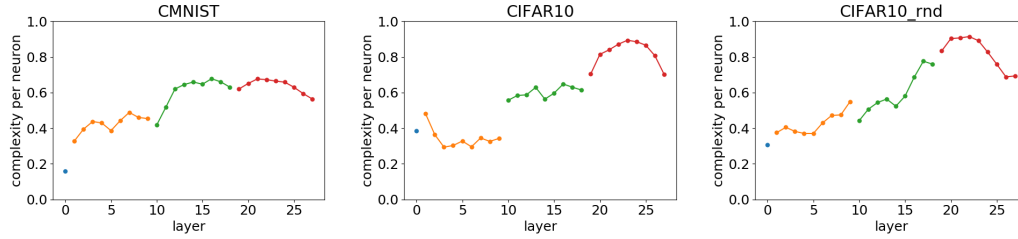


Figure 3: “Holographic” plot of the *complexity per neuron* as a function of layer depth (topmost ReLUs in residual cells).

5 Effective dimension

The particular definition of complexity introduced in section 4 measures the inherent *nonlinearity* of the operation of the neural network. It thus ignores any properties associated with the linear mode of operation of the network. But these are definitely very important for the understanding of the structure of feature representations. To this end we introduce the notion of an *effective dimension* of the feature representation of the given layer.²

Suppose that a layer has C output channels. We perform PCA of the C -dimensional layer output (understood as in section 3 in the convolutional case) obtaining the principle components and their appropriate variance ratio explained $p_i = \lambda_i / \sum_{i=1}^C \lambda_i$. In order not to set an arbitrary threshold for the variance ratio and yet measure an effective dimensionality of the output, we evaluate the entropy of p_i :

$$S[\{p_i\}] = - \sum_{i=1}^C p_i \log p_i \quad (9)$$

and define the effective dimension as

$$effective\ dimension = \exp(S[\{p_i\}]) \quad (10)$$

This definition reproduces the correct answer for simple cases like $p_1 = p_2 = \dots = p_k = 1/k$, $p_{i>k} = 0$ and interpolates naturally to others. Also it mimics the physical picture of entropy as the logarithm of the number of microstates.

6 Complexity and effective dimension for a deep convolutional neural network

In this section we perform experiments with a resnet-56 network (version for CIFAR-10 [29]). The network is structured as follows: an initial convolutional layer (block 1), then three blocks of 9 residual cells each, and an output layer following average pooling. The three blocks (block 2-4)

²A related notion was introduced in [28] where, in contrast to our case, an explicit threshold for the explained variance ratio was used together with average pooling over the whole image.

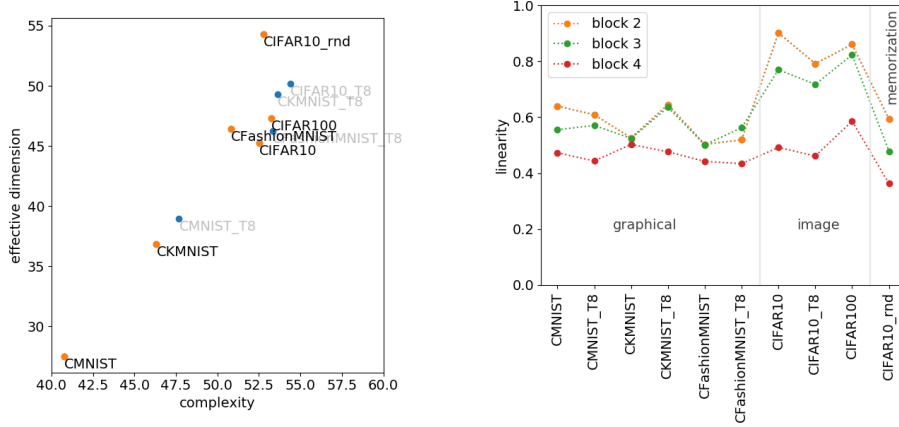


Figure 4: *Effective dimension* vs. *complexity* (averaged over the top block) for trained resnet-56 on various datasets (left). Average *linearity* for layers in the three successive blocks of resnet-56 for various datasets (right). The lines serve to guide the eye.

operate on resolutions 32×32 , 16×16 and 8×8 respectively and have 16, 32 and 64 channels. The variant of the residual cell used here has a ReLU right after summation. The second ReLU is in the residual branch. For the observables defined in sections 4 and 5 we collect the outputs after each ReLU. In the majority of cases we discuss the outputs of the ReLU after summation (to which we refer as the ‘topmost’ one). This can be understood as measuring the *complexity* and *effective dimension* of the whole residual cell treated as a single unit as it is exactly this output which goes into subsequent residual cells. The outputs are always evaluated on the test sets of the respective datasets apart from CIFAR-10 with randomized labels where we use a sample of 10000 images from the training data. The training protocol is the same for all datasets.³

Properties of trained networks. In Figure 2 we show the dependence of the *effective dimension* as a function of layer depth for CMNIST, CIFAR-10 and CIFAR-10 with randomized labels. One can clearly see a consistent relatively smooth profile of increasing dimensionality of the feature representations, even though the three distinct stages with different resolution have markedly different number of channels (16, 32 and 64 respectively). We can also see a significant rise in the dimensionality of the highest level feature representations with the difficulty of the task. The effective dimension for the memorization task is, on the other hand, quite low in the lower resolution stages of processing.

Figure 3 shows the corresponding plot with *complexities* normalized to the number of channels. Here we observe a much flatter behaviour on CMNIST with almost continuous normalized complexity/entropy, and an increase of the complexity per neuron as we go to higher stages of processing for the two image datasets. Note that in contrast to the *effective dimension*, *complexity* scales more naturally with the number of channels/neurons.

In order to see how the *effective dimensions* and *complexities* are correlated with the intuitive difficulty of the learning task, we plot these observables in Fig. 4 (left) for a selection of datasets. These observables (for the topmost ReLU) are averaged over the layers in the top block of the network, which encompasses the high level processing. We observe a clear correlation with the difficulty of the classical datasets. The teared up versions are also more to the top and right than the original ones as one would intuitively expect. An additional intriguing feature of this plot is the fact that the various datasets lie on a linear band in the *effective dimension-complexity* plane. This is not, however, an automatic feature of the defined observables as can be seen in an analogous plot for the ReLU’s in the residual branch (see Fig. S1 in the Supplementary materials).

In Fig. 4 (right) we plot the averaged *linearity* in the three successive blocks of layers for the various datasets. We see that for the image datasets the lower blocks operate at a higher linearity, while for the memorization task they revert back to the lower values. It is intriguing that at the highest level of processing (block 4) the mean linearity is approximately the same for all datasets, yet the complexities differ substantially. This suggest that the key difference is the fact that the higher level

³The only exception was that weight decay was set to zero for CIFAR-10 with randomized labels.

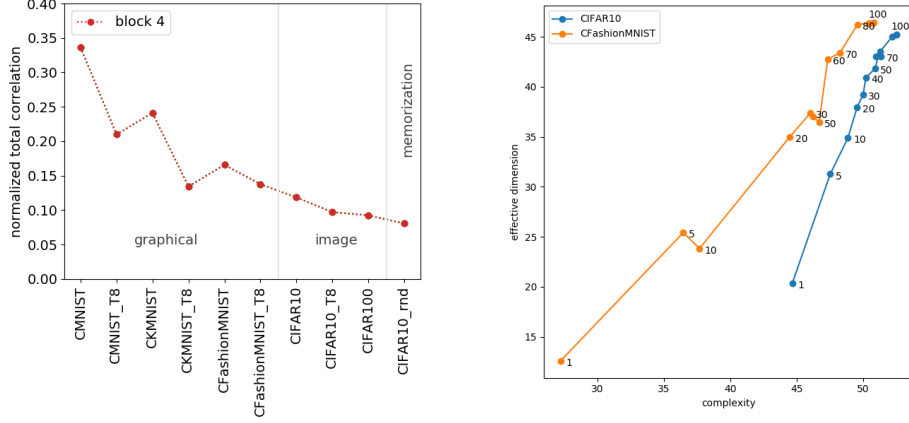


Figure 5: Normalized total correlation (topmost ReLUs) for trained resnet-56 on various datasets (left). Training trajectories in the *effective dimension* - *complexity* plane (right)

neurons operate in a much less correlated way for the more complicated datasets leading to a decrease of total correlation (7). Indeed such behaviour can be clearly seen in Fig. 5(left).

Finally, let us emphasize that one can interpret all the above observations from two points of view. On the one hand, one can gather insight into the finer details of how the deep neural network deals with the particular classification task. On the other hand, one can view these results as representing nontrivial information about the internal structure of each particular dataset at various scales.

The dynamics of training. As indicated in the introduction, it is very interesting to analyze the evolution of the introduced observables during the learning process. In Fig. 5 (right) we show the trajectories in the *effective dimension-complexity* plane for the topmost layers (block-4) for CFashionMNIST and CIFAR-10 datasets. We see that during training both observables steadily increase. Although, one should note that the *effective dimension* increases in a much more significant way. Thus during learning the network generates richer (effectively higher dimensional) high level representations.

In this context it is interesting to contrast this with the case of the memorization task i.e. CIFAR-10 with random labels. There, in the initial stages of learning, the dimensionality stays low while the complexity increases, and only later one gets a very sharp rise in the dimensionality (see Fig. S2 *Supplementary information*).

The above pictures represent the topmost ReLU in the residual cell – so the relevant signal which gets propagated to subsequent layers. The ReLU in the middle of the residual cell exhibits more varied behaviour with an increase of *effective dimension* but no clear directionality for *complexity* (see Fig. S3 *Supplementary information*).

We also analyzed the behaviour of linearity and total correlation during training on CIFAR-10. Of particular note is the strong reduction in the linearity of the residual layers, rather mild dependence for the topmost layers and the marked decrease in *total correlation* (see Figures S4-S5 *Supplementary information*). This last fact is especially interesting as it indicates that the neurons become more and more independent in the course of training, especially at the highest processing levels.

7 Fully Connected, Highway and small neural networks

Clearly the observables defined in the present paper may be investigated for a network of any size and architecture. In particular, in this section we present complementary investigations focused on entropic features in minimal fully connected networks, in order to be able to explore variability with the network size and possible novel phenomena for other architectures.

Shallow fully connected network. We consider a three-layer network (FC3) with the entry layer $L1$ fixed at 14 neurons and the size of the middle layer $L2$ varying in the range $N \in [4, 768]$. All

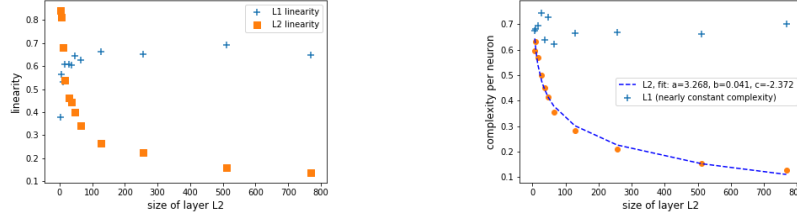


Figure 6: Average *linearity* scaling with $L2$ width N (left). *Complexity per neuron* scaling ($a/N^b + c$) of the second layer $L2$, with almost constant complexity of the first layer $L1$ in FC3 (right).

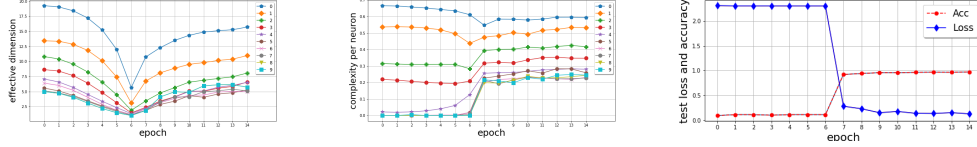


Figure 7: 11-layer 28 neuron wide Highway Network *effective dimension* (left), complexity per neuron of the nonlinear part (middle) and test accuracy and loss evaluation (right).

variants are trained on MNIST dataset to accuracy 95%. We find that the average *linearity* changes substantially with $L2$ width for both layers as seen in the Fig. 6 (left), even though the size of layer $L1$ is kept fixed. Interestingly, the *complexity per neuron* for layer $L2$ scales as a power law, whereas for $L1$ it does not really depend on the size of the subsequent layer (Fig. 6 (right)).

Highway networks. As an example of a deeper fully connected network with a nontrivial architecture we investigate an 11-layer, 28 neuron wide highway network [30]. We observe a very distinctive pattern, reminiscent of a phase transition, in the behaviour of both the *effective dimension* and non-linear outputs *complexity* during the course of training, which coincides with the abrupt transition around epoch 5 in the test loss and accuracy (see Fig. 7). Interestingly the behaviour of the various layers gets slightly desynchronised and shifted to earlier and later epochs, once one changes the depth/width of the network (see Fig. S6 *Supplementary information*). The dip/quench is not seen in the case of resnet-56, but can be observed in a small convolutional network at very low learning rate (see Fig. S7 *Supplementary information*).

8 Conclusions and outlook

In the present paper we defined two complementary observables which, in a quantitative way capture the properties of information processing and feature representations in an artificial neural network. *Complexity* is a measure of the inherent nonlinearity, while the *effective dimension* captures also properties of neurons acting in the linear regime. Both observables may be applied at the level of an individual layer and thus can quantify these properties as a function of scale.

Both observables pick out marked differences between datasets with an overall increase with the difficulty of the training task of the complexity and effective dimension of the highest level layers, but also provide more subtle insight, like the decrease of total correlation between neurons for more challenging datasets and a distinct dependence on scale (layer depth). The latter can be interpreted in a dual way as reflecting the internal structure of a dataset, with the deep neural network used just as a tool. We believe that this point of view opens up numerous directions for further research.

We also studied the dynamics of training, which exhibits a rise in the effective dimension of the feature representations (thus generating richer representations) as well as a decrease in total correlations, so that the high level neurons tend to operate more and more independently. We also demonstrated the use of these techniques on smaller networks, which can yield challenging data for our understanding of neural network dynamics.

Finally, it would be intriguing to understand, for a given dataset, what would be the smallest complexity of a neural network which achieves a given accuracy threshold.

Acknowledgements. This work was supported by the Foundation for Polish Science (FNP) project *Bio-inspired Artificial Neural Networks* POIR.04.04.00-00-14DE/18-00. We would like to thank Wojciech Tarnowski for pointing out ref. [28].

References

- [1] E. Schneidman, M.J. Berry II, R. Segev, W. Bialek, *Weak pairwise correlations imply strongly correlated network states in a neural population*, Nature 440 (2006) 1007.
G. Tkacik, E. Schneidman, M.J. Berry II, W. Bialek, *Ising models for networks of real neurons*, [arXiv:q-bio.NC/061107]
See also C. Zanoci, N. Dehghani, M. Tegmark, *Ensemble Inhibition and Excitation in the Human Cortex: an Ising Model Analysis with Uncertainties* Phys. Rev. E 99, 032408 (2019), [arXiv:1810.07253]
- [2] C. Zhang, S. Bengio, M. Hardt, B. Recht, O. Vinyals, *Understanding deep learning requires rethinking generalization* ICLR 2017, [arXiv:1611.03530]
- [3] S. Shalev-Shwartz, S. Ben-David, *Understanding Machine Learning: From Theory to Algorithms*, Cambridge 2014, ISBN: 9781107057135
- [4] K. Kawaguchi, L. Pack Kaelbling, and Y. Bengio, *Generalization in Deep Learning*, MIT-CSAIL-TR-2018-014 2017, [arXiv:1710.05468]
- [5] V. P. Roychowdhury, K. Y. Siu, A. Orlitsky, and T. Kailath, *On the Circuit Complexity of Neural Networks* in *Proceedings of the 1990 Conference on Advances in Neural Information Processing Systems 3*, pages 953–959, NIPS-3 1990.
- [6] I. Parberry, *Circuit Complexity and Feedforward Neural Networks* in *Mathematical Perspectives on Neural Networks (Developments in Connectionist Theory Series by P. Smolensky (Editor), M. C. Mozer (Editor), D.E. Rumelhart (Editor)*, 2004.
- [7] A. Novikov, D. Podoprikin, A. Osokin, and D. Vetrov, *Tensorizing Neural Networks*, 2015, [arXiv:1509.06569]
- [8] T. Garipov, D. Podoprikin, A. Novikov, and D. Vetrov, *Ultimate tensorization: compressing convolutional and FC layers alike*, 2016, [arXiv:1611.03214]
- [9] R. Orús, “Tensor networks for complex quantum systems,” APS Physics **1** (2019), 538-550, [arXiv:1812.04011]
- [10] P. Austrin, P. Kaski, and K. Kubjas, *Tensor network complexity of multilinear maps*, 2017, [arXiv:1712.09630]
- [11] N. Cohen, O. Sharir, and A. Shashua, *On the Expressive Power of Deep Learning: A Tensor Analysis*, 29th Annual Conference on Learning Theory, pp. 698-728, 2016, [arXiv:1509.05009]
- [12] N. Cohen, O. Sharir, Y. Levine, R. Tamari, D. Yakira, and A. Shashua, *Analysis and Design of Convolutional Networks via Hierarchical Tensor Decompositions*, 2017, [arXiv:1705.02302]
- [13] Y. Levine, D. Yakira, N. Cohen, and A. Shashua, *Deep Learning and Quantum Entanglement: Fundamental Connections with Implications to Network Design*, 2017, [arXiv:1704.01552]
- [14] D. Liu, S.-J. Ran, P. Wittek, C. Peng, R. B. García, G. Su, and M. Lewenstein, *Machine learning by unitary tensor network of hierarchical tree structure*, New Journal of Physics, Volume 21, July 2019, [arXiv:1710.04833]
- [15] A. Novikov, M. Trofimov and I. Oseledets, *Exponential Machines*, 2016, [arXiv:1605.03795]
- [16] E. Miles Stoudenmire, and D. J. Schwab, *Supervised Learning with Quantum-Inspired Tensor Networks*, 2016, [arXiv:1605.05775]
- [17] J. Molina-Vilaplana, A. del Campo, *Complexity functionals and complexity growth limits in continuous MERA circuits*, JHEP 08 012 (2018), [arXiv:1803.02356]
- [18] H.A. Camargo, M.P. Heller, R. Jefferson, J. Knaute, *Path integral optimization as circuit complexity*, Phys. Rev. Lett. 123, 011601 (2019), [arXiv:1904.02713]
- [19] J. M. Maldacena, “The Large N limit of superconformal field theories and supergravity,” Int. J. Theor. Phys. 38 (1999) 1113 [Adv. Theor. Math. Phys. 2 (1998) 231], [hep-th/9711200]
M. Natsuume, *AdS/CFT Duality User Guide*, Lect.Notes Phys. 903 (2015) pp.1-294, [arXiv:1409.3575]

- [20] K. Hashimoto, *AdS/CFT as a deep Boltzmann machine*, Phys. Rev. D 99, 106017 (2019), [arXiv:1903.04951]
K. Hashimoto, S. Sugishita, A. Tanaka, A. Tomiya, *Deep Learning and the AdS/CFT Correspondence.*, Phys. Rev. D 98, 046019 (2018), [arXiv:1802.08313]
- [21] B. Swingle, “Entanglement Renormalization and Holography,” Phys. Rev. D 86 (2012) 065007, [arXiv:0905.1317]
- [22] R. Orús, *Advances on tensor network theory: symmetries, fermions, entanglement, and holography*, Eur. Phys. J. B 87, 280 (2014), [arXiv:1407.6552]
- [23] D. Stanford, L. Susskind, *Complexity and Shock Wave Geometries*, Phys. Rev. D 90, 126007 (2014), [arXiv:1406.2678]
- [24] R. Landauer, *Irreversibility and Heat Generation in the Computing Process*, in *IBM Journal of Research and Development*, vol. 5, no. 3, pp. 183-191, July 1961, doi: 10.1147/rd.53.0183.
- [25] H.C. Nguyen, R. Zecchina, J. Berg, *Inverse statistical problems: from the inverse Ising problem to data science*. Advances in Physics, 66 (3), 197-261 (2017), [arXiv:1702.01522]
- [26] R.A. Janik, *Entropy from Machine Learning*, [arXiv:1909.10831]
- [27] T. Chen, C. Guestrin, *XGBoost: A Scalable Tree Boosting System*, [arXiv:1603.02754]
- [28] J. Shenk, M.L. Richter, A. Arpteg, M. Huss, *Spectral Analysis of Latent Representations*, [arXiv:1907.08589]
- [29] K. He, X. Zhang, S. Ren, J. Sun, *Deep Residual Learning for Image Recognition*, CVPR 2016, [arXiv:1512.03385]
- [30] R.K. Srivastava, K. Greff and J. Schmidhuber, *Highway Networks*, 2015, [arXiv:1505.00387]

Supplementary information

Training parameters

All the experiments performed with resnet-56 were trained with the same settings: 100 epochs, SGD optimizer with the learning rate equal to 0.1, weight decay equal to 0.0001 (it was set exceptionally to 0 for CIFAR-10 with randomized labels), batch size 128 (settings typical for CIFAR-10). Learning rate was reduced by a factor of 10 at the 80th and 90th epochs. In order to make a comparison with other datasets, so that any differences would only be due to the character of the learning task, we did not alter the training settings even for the much simpler datasets like CMNIST.

The only exception was setting weight decay to zero for the memorization task i.e. CIFAR-10 with randomized labels, as that task is very peculiar in its character. In general we may expect high variability in that case, so the results should be understood as showing a particular realization for memorization.

The code was a modified version of the implementation provided by Yerlan Idelbayev in https://github.com/akamaster/pytorch_resnet_cifar10.

The train/test splits were the standard ones for CIFAR-10, MNIST, KMNIST and FashionMNIST. For CIFAR-10 with random labels we only used the training part of CIFAR-10.

The networks used in Section 7 had the following training parameters:

All small models were trained on MNIST with batch size 64. The simplest three layer networks FC3 were trained for a range of layer widths described in the main text. Models were optimised with Adadelata adaptive algorithm with initial learning rate 1 for 10 epochs, where observables were measured.

Highway Networks were trained using Adadelata optimiser and initial learning rate 0.8 for 15 epochs.

Small convolutional network had topology [4-8-8]-[64-32-10] (three Conv2D layers of specified depth and two FC layers of classifier followed by output) with kernel size 3x3, stride 1, MaxPooling and again Adadelata optimiser with initial learning rate 0.0003 for 15 epochs.

Entropy computation

The entropy computation using xgboost used a 2-fold split instead of the default 5-fold from <https://github.com/rmldj/ml-entropy> in order to reduce computation time. The settings were `n_estimators=100`, `max_depth=3` and `learning_rate=0.1` (defaults for xgboost version 0.90, note that the defaults changed in subsequent versions). The employed method of computing entropy estimates the entropy which cannot be explained using a given classifier (see the original paper <https://arxiv.org/abs/1909.10831> for details). Hence we keep the same settings for the classifier for the various datasets so that the entropy estimates are comparable.

Note that these entropy estimates should be treated as bounds from above on the entropy (see the referenced paper) and could in principle be lowered by refining the settings of the classifier. We refrained from doing that as the computation of the entropies for all layers of resnet-56 is very time consuming (more than 5 hours on a powerful 6-core desktop (12 threads) for a single model/epoch of interest) and we were mostly interested in *relative* comparisons between the entropies/complexities for various datasets.

Computing time considerations and infrastructure

As the computation of the entropy is very time consuming, we refrained from performing repeated trainings and evaluations, especially as our focus was to exhibit clear *qualitative* behaviours as well as depth-wise profiles for *particular* trained networks. The simulations were done using GTX970, GTX980 and GTX2080 Ti graphics cards.

Datasets

In this work we investigate the same deep convolutional neural network trained on a variety of datasets of differing difficulty. Since our base network is adapted to CIFAR-10 with 32×32 colored images,

we made randomly colored versions (indicated by a prefix ‘C’) of the classical MNIST, KMNIST and FashionMNIST datasets. The original 28×28 images are randomly embedded into the 32×32 square and some random color noise is added to the objects (see Fig. 1 (left) in the main text).

In addition we formed teared up versions of all these datasets (with a suffix ‘_T8’) by cutting the original image into 8×8 pieces, randomly shuffling them and performing rotations by random multiples of 90° . We keep the choice of these random permutations and rotations *fixed and identical* for all images in a dataset. The motivation for this construction is that it makes a given dataset more challenging, while preserving the local features but upsetting the high-level global structure. The process is illustrated in Fig. 1 (right) in the main text.

We also use CIFAR-10 with randomized labels which represents a memorization task – memorizing the contents of 10 randomly chosen groups of images.

These datasets were implemented as PyTorch transformations. We will make them available on [github](#).

Supplementary figures for section 6

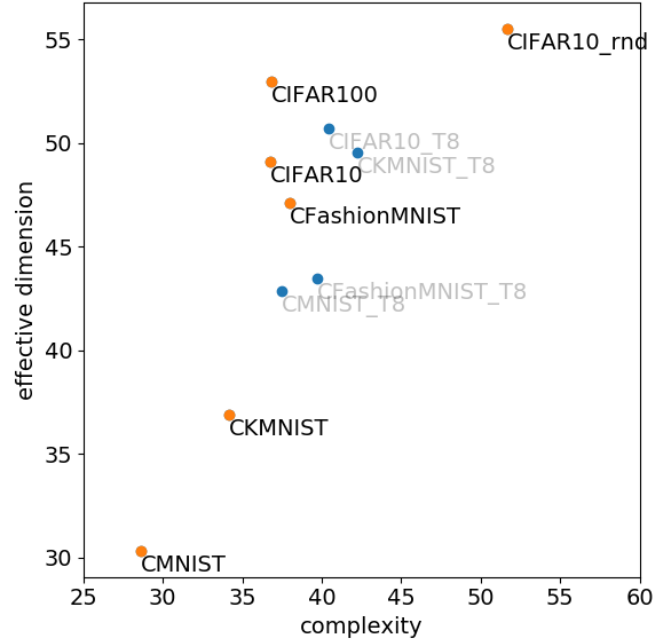


Figure S1: *Effective dimension* vs. *complexity* for the ReLU in the *residual branch* (averaged over the top block) for trained resnet-56 on various datasets.

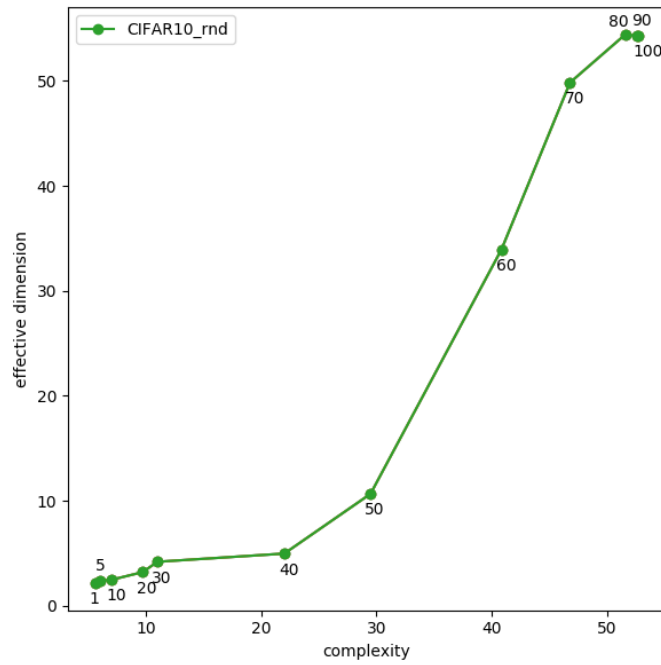


Figure S2: Training trajectories in the *effective dimension* - *complexity* plane for the memorization task – CIFAR-10 with random labels

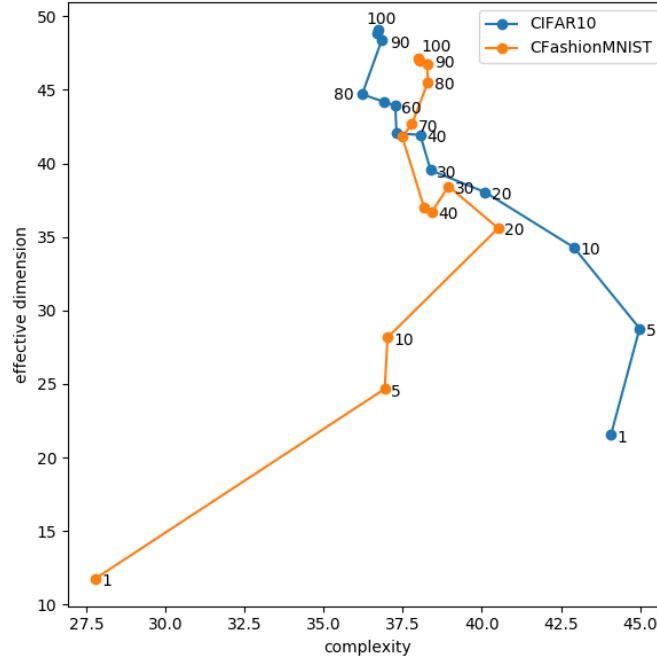


Figure S3: Training trajectories in the *effective dimension - complexity* for the ReLU in the residual cells of the final stage of the network.

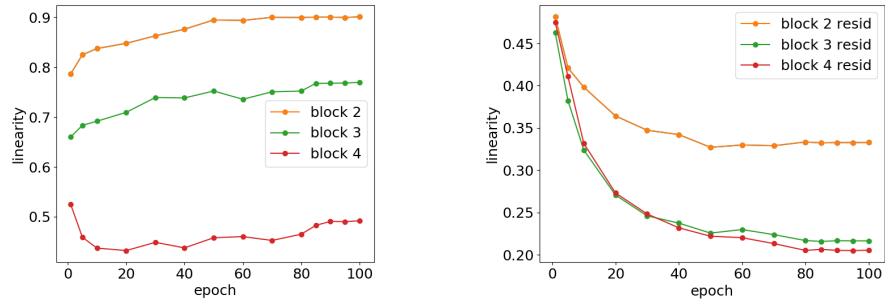


Figure S4: Averaged *linearity* in the top (left) and residual layers (right) during training on CIFAR-10.

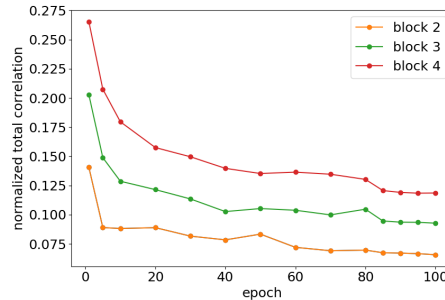


Figure S5: *Normalized total correlation* (topmost ReLU) during training on CIFAR-10.

Supplementary Figures and discussion for section 7

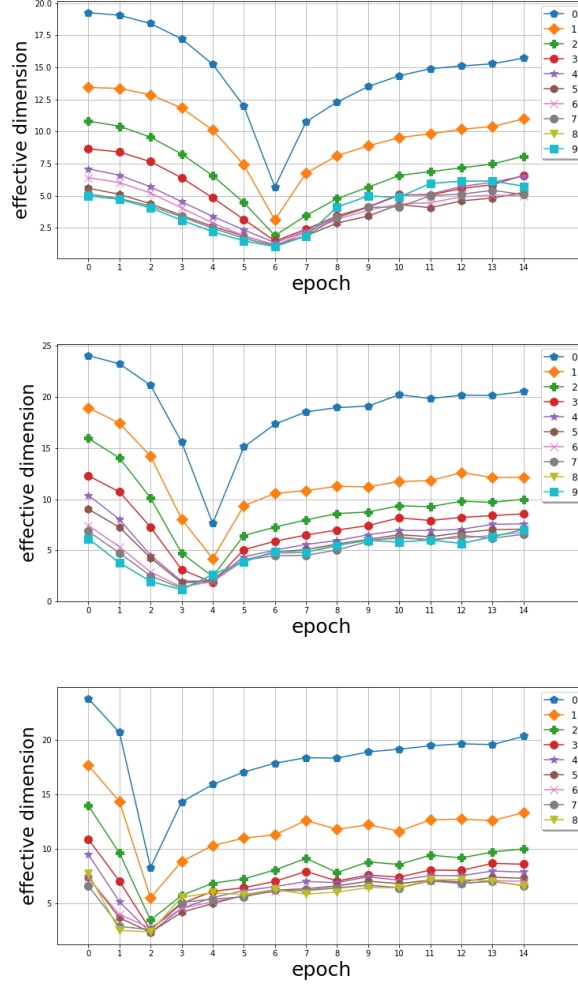


Figure S6: Highway Network *effective dimensions*: 11 layers, $N=28$ (*top*), 11 layers, $N=36$ (*middle*), 10 layers, $N=36$ (*bottom*). The minima are localised around the epoch of abrupt loss and accuracy jump (see main text, Section 7). Layers are numbered from the input. Output layer not shown.

More on Highway Networks. Highway Networks offer depth of deep models and flexibility of fully connected networks. These models are thus suitable to study entropic observables behaviour under depth and width variations. In Figure S6 we present three evolutions of *effective dimension* in the course of Highway Network training, with 11 layers deep, $N=28$, $N=36$ wide models as well as 10 layers deep, $N=36$ wide model. In all cases one observes collective quench in the observable, with details like minima synchronisation and locus sensitive to model parameters.

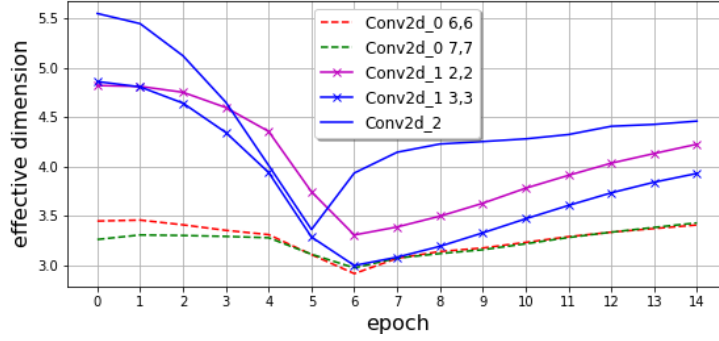


Figure S7: CNN pixel-wise *effective dimension* evolution of the three Conv2d layers. Comma separated numbers indicate pixel positions in the layer output feature maps.

Small convolutional network. Finally to check if similar behaviour in *effective dimension* can be observed in convolutional layer we have followed its evolution in a small CNN (see section *Training parameters* for the details of the architecture) with kernel size 3×3 trained on MNIST, to keep the dataset complexity fixed for comparison. Depicted in Figure S7 are transitions in *effective dimension* computed on one-pixel slices through all filters of the given Conv2d layer. The last Conv2d_2 is just a single 1×1 vector of channels and for two earlier layers we chose two indicated output pixel locations. As seen here, we again observe something akin to the behaviour present above in Fig. S6. Interestingly, the *effective dimension* does not settle even in the asymptotic, late learning region. The various Conv2d layer minima at different locations have different magnitudes (but are still synchronised), indicating diverse complexity across feature maps.